

## ATP13A3 is a major component of the enigmatic mammalian polyamine transport system

Norin Nabil Hamouda<sup>1</sup>, Chris Van den Haute<sup>2,3</sup>, Roeland Vanhoutte<sup>4</sup>, Ragna Sannerud<sup>5</sup>, Mujahid Azfar<sup>1</sup>, Rupert Mayer<sup>6</sup>, Álvaro Cortés Calabuig<sup>7</sup>, Johannes V. Swinnen<sup>8</sup>, Patrizia Agostinis<sup>9,10</sup>, Veerle Baekelandt<sup>2</sup>, Wim Annaert<sup>5</sup>, Francis Impens<sup>6</sup>, Steven H. L. Verhelst<sup>4,11</sup>, Jan Eggermont<sup>1</sup>, Shaun Martin<sup>1,#</sup>, Peter Vangheluwe<sup>1,#\*</sup>

<sup>1</sup> Laboratory of Cellular Transport Systems, <sup>4</sup> Laboratory of Chemical Biology, <sup>9</sup> Laboratory of Cell Death Research & Therapy, Department of Cellular and Molecular Medicine, KU Leuven, Leuven, Belgium

<sup>2</sup> Laboratory for Neurobiology and Gene Therapy, <sup>5</sup> VIB-KU Leuven Laboratory of Membrane Trafficking; Department of Neurosciences, KU Leuven, Leuven, Belgium

<sup>3</sup> Leuven Viral Vector Core, KU Leuven, Leuven, Belgium

<sup>6</sup> VIB Center for Medical Biotechnology, VIB Proteomics Core, Department for Biomolecular Medicine, Ghent University, Ghent, Belgium

<sup>7</sup> Genomics Core Leuven, KU Leuven, Leuven, Belgium

<sup>8</sup> Laboratory of Lipid Metabolism and Cancer, Department of Oncology, LKI – Leuven Cancer Institute, KU Leuven, Leuven, Belgium

<sup>10</sup> VIB-KU Leuven Center for Cancer Biology, Department of Oncology, KU Leuven, Leuven, Belgium

<sup>11</sup> Leibniz Institute for Analytical Sciences ISAS, Otto-Hahn-Str. 6b, 44227 Dortmund, Germany

# Joint last authors

**\* Corresponding author:**

Prof. Dr. Peter Vangheluwe

Department of Cellular and Molecular Medicine

KU Leuven Campus Gasthuisberg, O&N I Herestraat 49 - box 802, 3000 Leuven

Tel.: ±32 16 33 07 20

E-mail: [peter.vangheluwe@kuleuven.be](mailto:peter.vangheluwe@kuleuven.be)

ORCID ID: <https://orcid.org/0000-0002-7822-2944>

**Running Title:**

ATP13A3 is involved in Polyamine Transport

## List of contents

### **Supporting Information Figures**

- Figure S1. Polyamine biosynthesis pathway and its inhibitors.
- Figure S2. Effect of polyamines on viability of CHO-MG cells.
- Figure S3. ATP13A3 is downregulated in CHO-MG cells.
- Figure S4. Uptake of BODIPY-PUT uptake falls within the linear phase.
- Figure S5. Competition of MGBG with SPD and SPM in CHO-WT cells.
- Figure S6. Expression of wild-type ATP13A2 restores polyamine uptake, but it does not affect MGBG resistance in CHO-MG cells.

## Supporting Information Figures

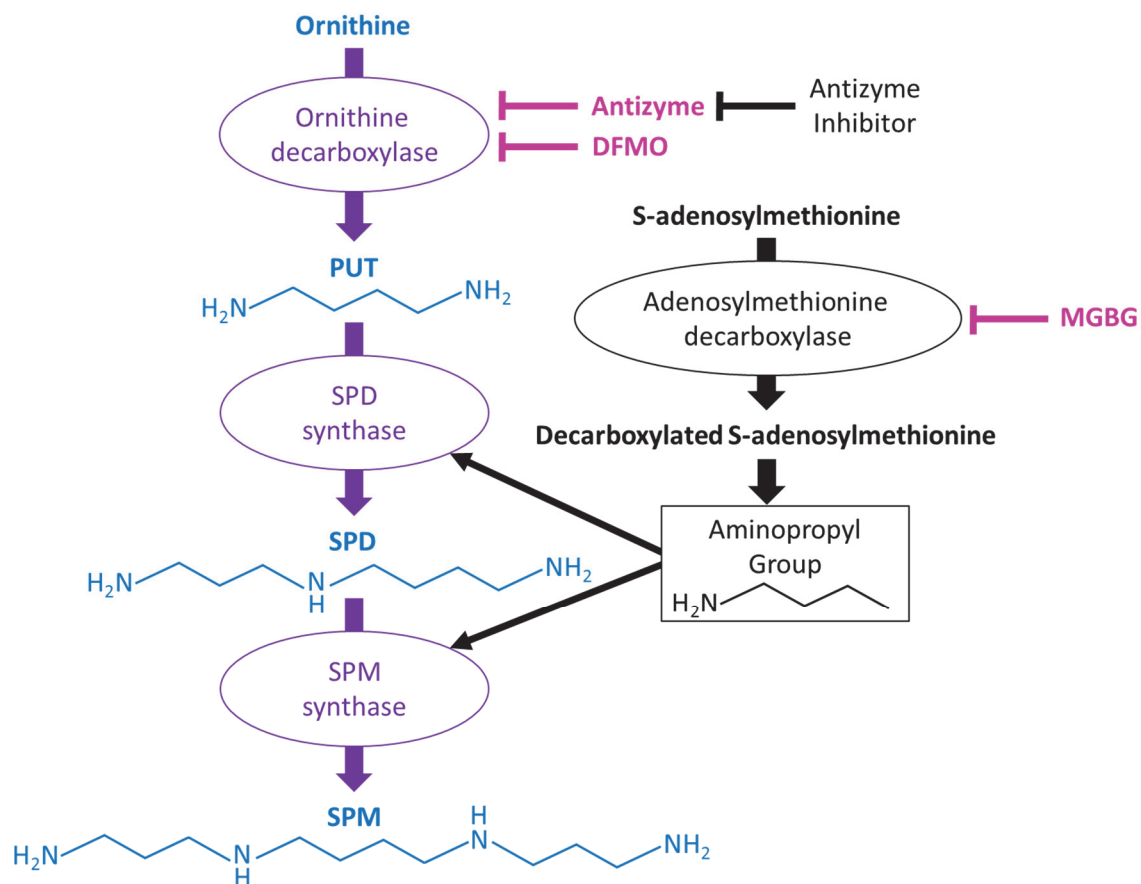


**Figure S1. Polyamine biosynthesis pathway and its inhibitors.** DFMO, difluoromethylornithine; MGBG, methylglyoxal bis-(guanyl hydrazone); SPM, spermine; SPD, spermidine; PUT, putrescine

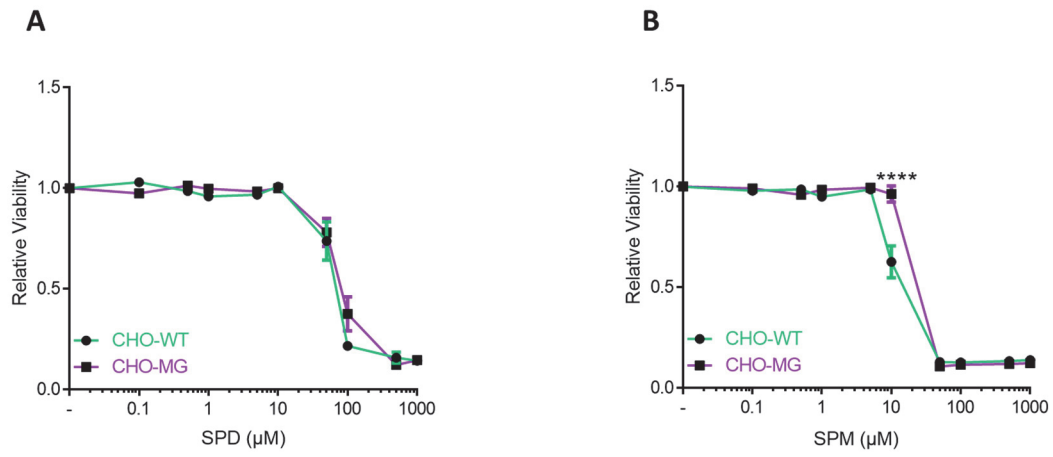


**Figure S2. Effect of polyamines on the viability of CHO-MG cells.** *A, B*, Cells were treated for 24 h with the indicated concentrations of only SPD (*A*) and SPM (*B*). CellTiter 96<sup>®</sup> AQueous One Solution Cell Proliferation Assay (MTS) was used to assess cell viability and dose-response curves were plotted (n=3). Data represent mean ± SEM (\*\*\*\**P*<0.0001) generated with two-way ANOVA and Bonferroni *post hoc* corrections. **SPM**, spermine; **SPD**, spermidine.

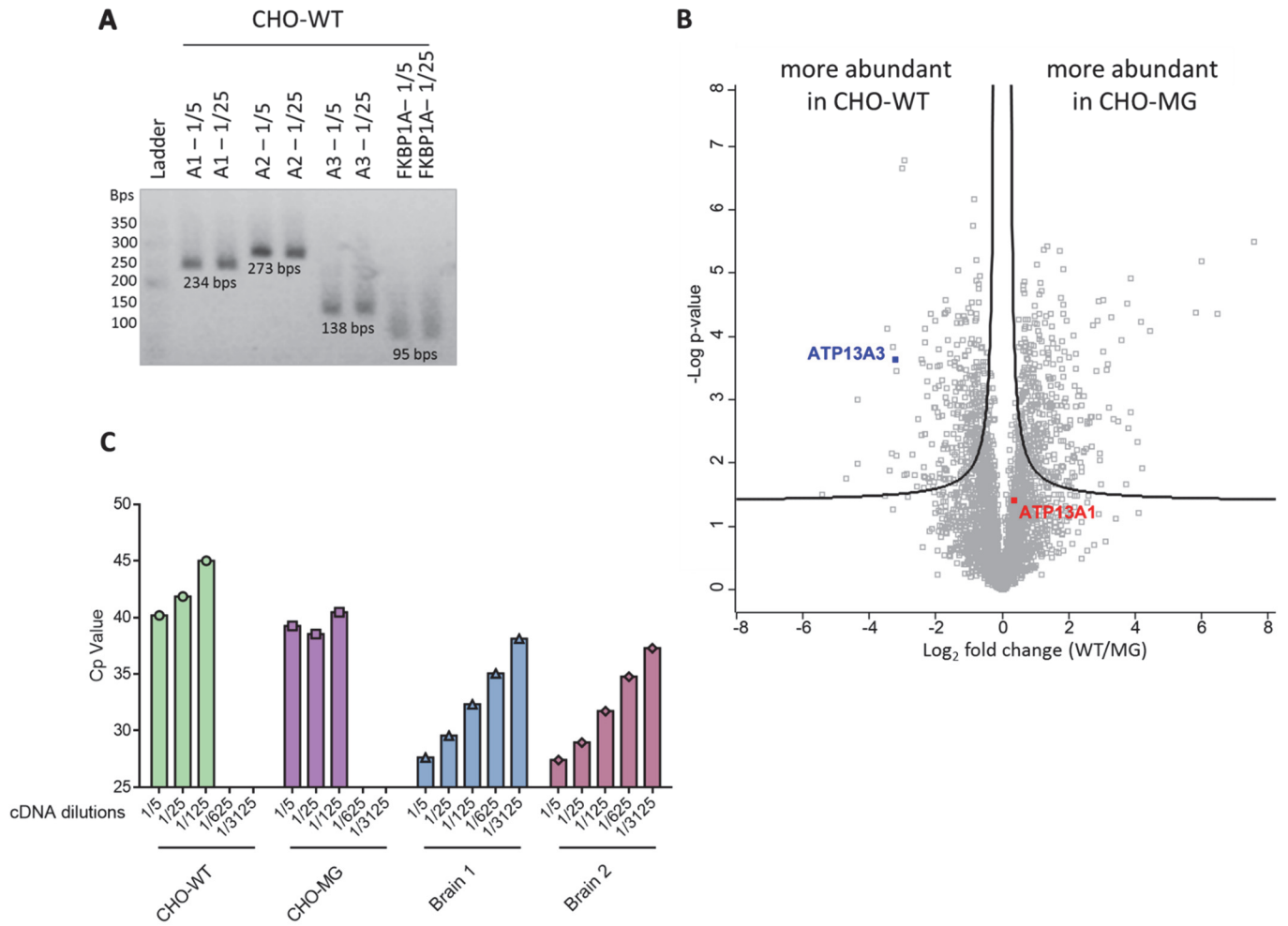


**Figure S3. ATP13A3 is downregulated in CHO-MG cells.** *A*, ATP13A1-3 mRNA levels were measured with qPCR using SYBR Green master mix and qPCR products from two cDNA dilutions (1/5, 1/25) were run on an agarose gel to check the specificity of the primers. *B*, Proteomic analysis was carried out on membrane fractions of CHO-WT and CHO-MG cells and detected proteins including ATP13A3 were plotted in a volcano plot (n=4). *C*, Cp values, demonstrating the ATP13A4 mRNA primer linearity in hamster brain tissues *versus* the CHO cells, are shown across the indicated cDNA dilutions. **A1-A3**, ATP13A1-3; **FKBPA1**, FKBP prolyl isomerase 1A

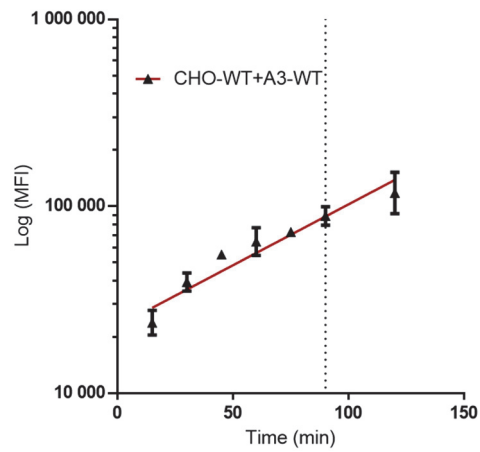


**Figure S4. Uptake of BODIPY-PUT uptake falls within the linear phase.** Cells were treated with 5  $\mu$ M BODIPY-PUT at 37°C for the indicated times. Uptake was measured in terms of mean fluorescence intensity (MFI) up to  $1 \times 10^4$  events (debris-free) per condition on the flow cytometer. Data represent mean  $\pm$  SEM. The dashed line refers to the time point that was used for the treatment of BODIPY-polyamines in all flow cytometry experiments (n=2-4). **A3-WT**, overexpression of wild type ATP13A3; **A3-DN**, overexpression of ATP13A3 catalytically dead mutant D498N; **BODIPY**, boron dipyrromethene; **PUT**, putrescine

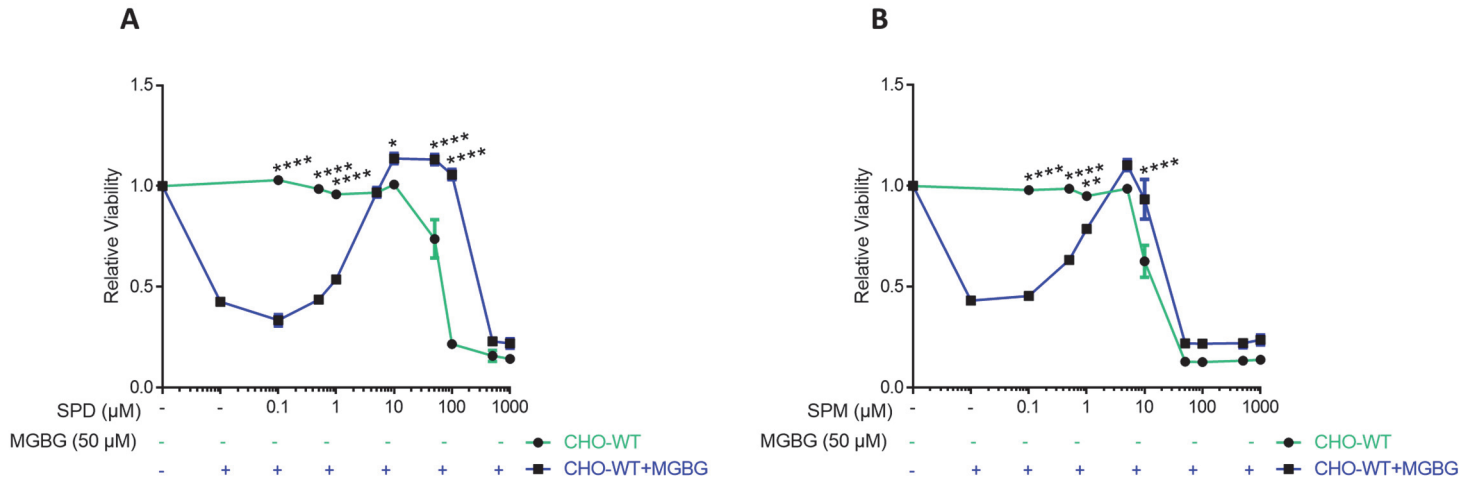


**Figure S5. Competition of MGBG with SPD and SPM in CHO-WT cells.** *A, B*, Cells were treated for 24 h with the indicated concentrations of SPD (n=3) (*A*) and SPM (n=3) (*B*) with or without 50 μM MGBG co-treatment. CellTiter 96<sup>®</sup> AQ<sub>ueous</sub> One Solution Cell Proliferation Assay (MTS) was used to assess cell viability and dose-response curves were plotted. Data represent mean ± SEM (\**P*<0.05, \*\**P*<0.01, \*\*\**P*<0.001, and \*\*\*\**P*<0.0001) generated with two-way ANOVA and Bonferroni *post hoc* corrections. **MGBG**, methylglyoxal bis-(guanyl hydrazone); **SPM**, spermine; **SPD**, spermidine

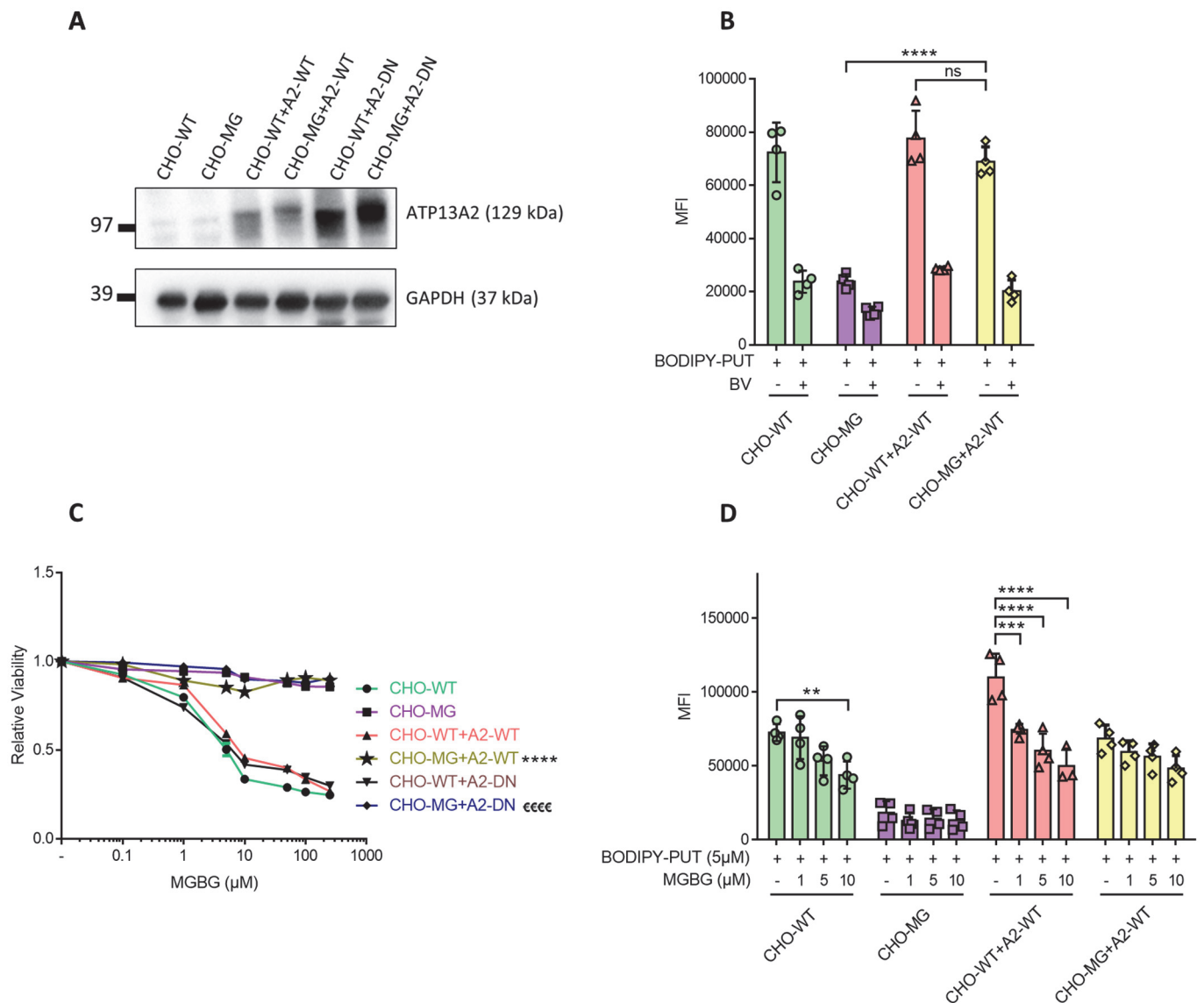


**Figure S6. Expression of wild-type ATP13A2 restores polyamine uptake, but it does not affect MGBG resistance in CHO-MG cells.** *A*, Stable cell lines were generated by lentiviral transduction to overexpress wild type (A2-WT) or a catalytically dead mutant (A2-DN) of ATP13A2. Expression of the viral vectors was verified by immunoblotting using ATP13A2 selective antibody, while the loading was monitored by house-keeping protein GAPDH selective antibody. *B*, *D*, Cells were treated with 5  $\mu\text{M}$  BODIPY-PUT alone (*B*) or combined with MGBG (*D*) for 90 min at 37°C with or without 90 min of 1 mM BV pre-treatment to inhibit polyamine uptake. Uptake was measured in terms of mean fluorescence intensity (MFI) up to  $1 \times 10^4$  events (debris-free) per condition on the flow cytometer ( $n=4$ ). *C*, Cells were treated for 24 h with different doses of MGBG. Cell viability was assessed using CellTiter 96<sup>®</sup> AQueous One Solution Cell Proliferation Assay (MTS) and dose-response curves were plotted ( $n=3$ ). Data represent or mean  $\pm$  SD (*B*, *D*) and individual data points (representing replicates) are overlaid on bar graph plots, or mean  $\pm$  SEM (*C*) (\*\* $P<0.01$ , \*\*\*\*<sup>eeee</sup> $P<0.0001$ , ns = not significant, \*\*\*\* vs CHO-WT+A2-WT, and eeee vs CHO-WT+A2-DN). Analyses were performed using two-way ANOVA and Bonferroni post hoc corrections. **BODIPY**, boron dipyrromethene; **BV**, benzyl viologen; **GAPDH**, Glyceraldehyde 3-phosphate dehydrogenase; **MGBG**, methylglyoxal bis-(guanyl hydrazone); **PUT**, putrescine; **A2-WT**, overexpression of wild type ATP13A2; **A2-DN**, overexpression of ATP13A2 catalytically dead mutant D508N